Stem Cell Reports
Report
ISSCR
OPEN ACCESS

Depletion of *Trp53* and *Cdkn2a* Does Not Promote Self-Renewal in the Mammary Gland but Amplifies Proliferation Induced by TNF-α

Linda J. van Weele,[1] Ferenc A. Scheeren,[1,3] Shang Cai,[1,4] Angera H. Kuo,[1] Dalong Qian,[1] William H.D. Ho,[1,2] and Michael F. Clarke[1,*]

[1]Institute for Stem Cell Biology and Regenerative Medicine, School of Medicine, Stanford University, Stanford, CA, USA
[2]Department of Stem Cell Biotechnology, California State University Channel Islands, Camarillo, CA, USA
[3]Present address: Department of Medical Oncology, Leiden University Medical Center, Leiden, the Netherlands
[4]Present address: Westlake University, Shilongshan Street No. 18, Xihu District, Hangzhou, Zhejiang Province, China
*Correspondence: mfclarke@stanford.edu
https://doi.org/10.1016/j.stemcr.2020.12.012

SUMMARY

The mammary epithelium undergoes several rounds of extensive proliferation during the female reproductive cycle. Its expansion is a tightly regulated process, fueled by the mammary stem cells and these cells' unique property of self-renewal. Sufficient new cells have to be produced to maintain the integrity of a tissue, but excessive proliferation resulting in tumorigenesis needs to be prevented. Three well-known tumor suppressors, p53, $p16^{INK4a}$, and $p19^{ARF}$, have been connected to the limiting of stem cell self-renewal and proliferation. Here we investigate the roles of these three proteins in the regulation of self-renewal and proliferation of mammary epithelial cells. Using mammary epithelial-specific mouse models targeting *Trp53* and *Cdkn2a*, the gene coding for $p16^{INK4a}$ and $p19^{ARF}$, we demonstrate that p53, $p16^{INK4a}$, and $p19^{ARF}$ do not play a significant role in the limitation of normal mammary epithelium self-renewal and proliferation, whereas in the presence of the inflammatory cytokine TNF-α, $Trp53^{-/-}$ $Cdkn2a^{-/-}$ mammary basal cells exhibit amplified proliferation.

INTRODUCTION

The epigenetic regulator Bmi1 represses differentiation in various tissue-specific stem cells, such as hematopoietic stem cells (Lessard and Sauvageau, 2003; Park et al., 2003; Rizo et al., 2009) and mammary stem cells (Pietersen et al., 2008). Bmi1 targets *Cdkn2a*, a gene containing the reading frames for $p16^{INK4A}$ and $p14^{ARF}$ in humans and $p16^{INK4a}$ and $p19^{ARF}$ in mice that play an essential role in the induction of senescence and cell-cycle arrest. $p16^{INK4A}$/$p16^{INK4a}$ inhibits cell-cycle progression from G1 to S phase. $p14^{ARF}$/$p19^{ARF}$ inhibits MDM2/Mdm2, leading to activation of p53. p53, $p16^{INK4a}$, and $p19^{ARF}$ respond to stress signals and induce cell-cycle arrest and apoptosis. Their ability to halt cell division prevents uncontrolled proliferation in tissues that can lead to tumor growth (Charni et al., 2017; Lowe and Sherr, 2003).

Within the hematopoietic system, simultaneously deleting *Cdkn2a* and *Trp53* leads to a 10-fold increase in the number of cells able to self-renew and provides multipotent progenitors with self-renewing capacity, a property normally attributed only to stem cells (Akala et al., 2008). In the mammary gland, various groups have deleted *Trp53* or *Cdkn2a*, but not both, and examined the effect on self-renewal (Chiche et al., 2013; Cicalese et al., 2009; Pietersen et al., 2008; Tao et al., 2011). To our knowledge, no studies have investigated the effect, especially on self-renewal, of deleting these genes concurrently in the mammary gland.

Here, using our epithelial-specific mouse model, we demonstrate that p53, $p16^{INK4a}$, and $p19^{ARF}$ do not play a significant role in the regulation of mammary epithelium self-renewal and proliferation in C57BL/6J mice. In a primary transplantation assay used to study short-term self-renewal, depletion of the three tumor suppressors does not affect the number of regenerating cells nor their proliferative capacity under normal physiologic conditions. Long-term self-renewal, evaluated using a secondary transplantation assay, also shows no effect on proliferation. In addition, tumor suppressor deletion does not affect long-term self-renewal in mammary epithelial cells (MECs) compared with the control; however, $Trp53^{-/-}$ cells show a decrease in regenerating cells compared with $Trp53^{-/-}$ $Cdkn2a^{-/-}$ cells. RNA expression analysis suggests that TNF-α-dependent signaling is upregulated in $Trp53^{-/-}$ $Cdkn2a^{-/-}$ mammary epithelial basal cells. *In vitro*, we find that TNF-α increases organoid formation and proliferation in wild-type (WT) and $Trp53^{-/-}$ $Cdkn2a^{-/-}$ basal MECs; however, compared with WT MECs, $Trp53^{-/-}$ $Cdkn2a^{-/-}$ basal MECs are sensitized to TNF-α-induced proliferation.

RESULTS

Generation of *Cdkn2a* Knockout and/or *Trp53* Knockout Mouse Models

To investigate the effect of p53, $p16^{INK4a}$, and $p19^{ARF}$ on self-renewal and proliferation, we generated multiple loss-of-function mouse models. Female mice with homozygous germline combined deletions of *Cdkn2a* and *Trp53* are inviable. Therefore, we crossed the *Cdkn2a* null mouse (Serrano et al., 1996) with a conditional $Trp53^{flox}$ ($Trp53^{f}$)

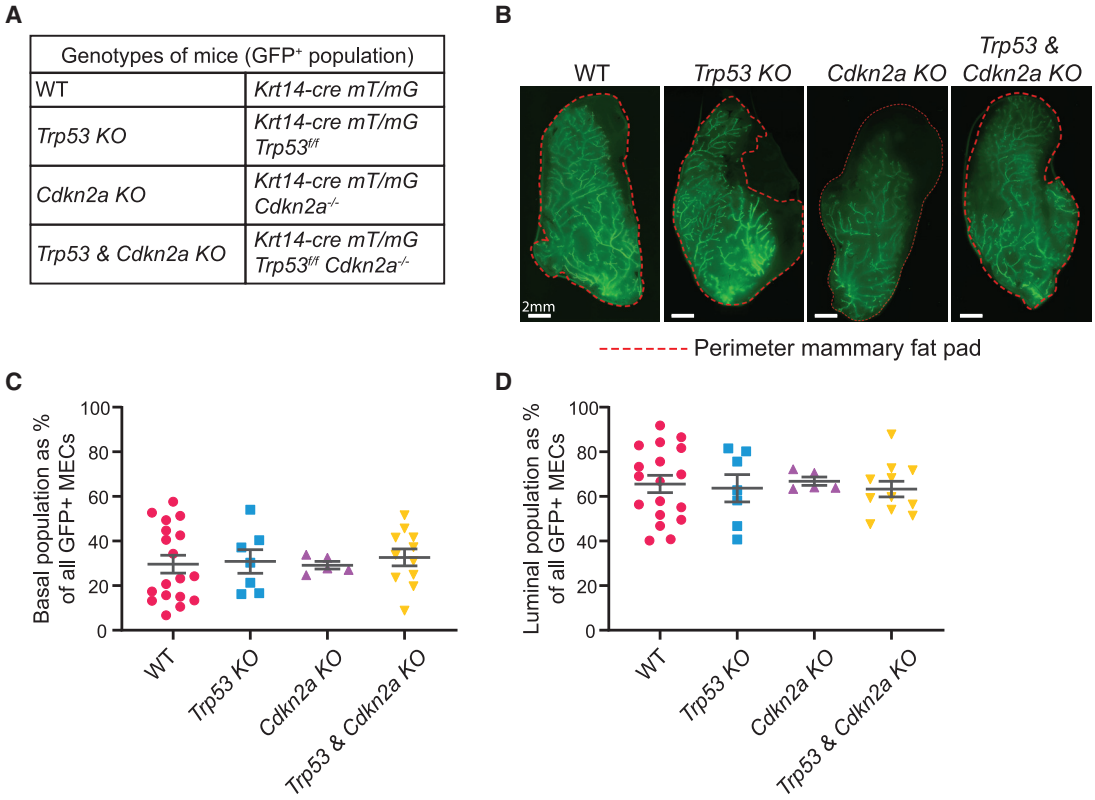

Figure 1. MECs Develop Similarly in WT, *Trp53 KO*, *Cdkn2a KO*, and *Trp53 & Cdkn2a KO* Mice

(A) Tabular overview of the abbreviations used for the four different transgenic mice described in this study. In Figure S1, the gating strategy used for FACS throughout this study (Figure S1A) and an analysis of the efficiency of the Cre-lox system (Figures S1B and S1C) are displayed.

(B) Representative fluorescence images of WT, *Trp53 KO*, *Cdkn2a KO*, and *Trp53 & Cdkn2a KO* mammary glands. Mammary epithelial cells are marked by GFP. Fat pads were freshly dissected from mice and photographed.

(C and D) Flow cytometry analysis shows the percentage of WT, *Trp53 KO*, *Cdkn2a KO*, and *Trp53 & Cdkn2a KO* basal (C) and luminal (D) cells. Data are presented as mean ± SEM; each symbol represents data derived from one mouse ($p > 0.05$ for all comparisons; one-way ANOVA).

mouse (Jonkers et al., 2001). Loss of *Trp53* was induced by the *Krt14-Cre* transgene (Dassule et al., 2000). *Krt14* is expressed in all MECs during embryonic development (Sun et al., 2010; Van Keymeulen et al., 2011). To visually mark cells that lost *Trp53*, we introduced the *mT/mG* transgene (Muzumdar et al., 2007). Cre excises *mT/mG's tdTomato* allele and activates the expression of *GFP* simultaneously, indicating the excision of *Trp53*. We used flow cytometry to confirm the efficiency of specificity of *Krt14-Cre*. In accordance with a previous publication (Mitchell and Serra, 2014), flow cytometry showed that 99.8% of all GFP^+ cells are in the luminal and basal populations (Figures S1A and S1B). Subsequently, real-time qPCR confirmed the absence of *Trp53* in basal and luminal GFP^+ populations (Figure S1C). The various crosses lead to the four following mouse models, which are used in these studies: (1) WT, *Krt14-Cre mT/mG*; (2) *Trp53 KO* (knockout), *Krt14-Cre mT/mG Trp53*$^{f/f}$; (3) *Cdkn2a KO*, *Krt14-Cre mT/mG Cdkn2a*$Cd^{-/-}$; and (4) *Trp53 & Cdkn2a KO*, *Krt14-Cre mT/mG Trp53*$^{f/f}$ *Cdkn2a*$^{-/-}$ (Figure 1A).

Endogenous MECs Develop Similarly in All Mutant Mouse Models

The mammary glands of female adult WT, *Trp53 KO*, *Cdkn2a KO*, and *Trp53 & Cdkn2a KO* mice showed no differences in branch development (Figure 1B). Moreover, the percentages of cells contributing to the basal and luminal populations were equal as determined by flow cytometry (Figures 1C and 1D). These data show that depleting MECs of *Cdkn2a* and/or *Trp53* neither results in differences in the phenotypic duct formation nor affects the ratio of basal to luminal cells.

MECs in All Mutant Mouse Models Display Equal Short-Term Regenerative and Proliferative Efficiency in Primary Transplantation Assay

To determine the frequency of cells able to reconstitute the mammary gland, we performed a mammary gland limiting dilution transplantation assay in syngeneic mice (Figure S2). The repopulation frequency is comparable between MECs

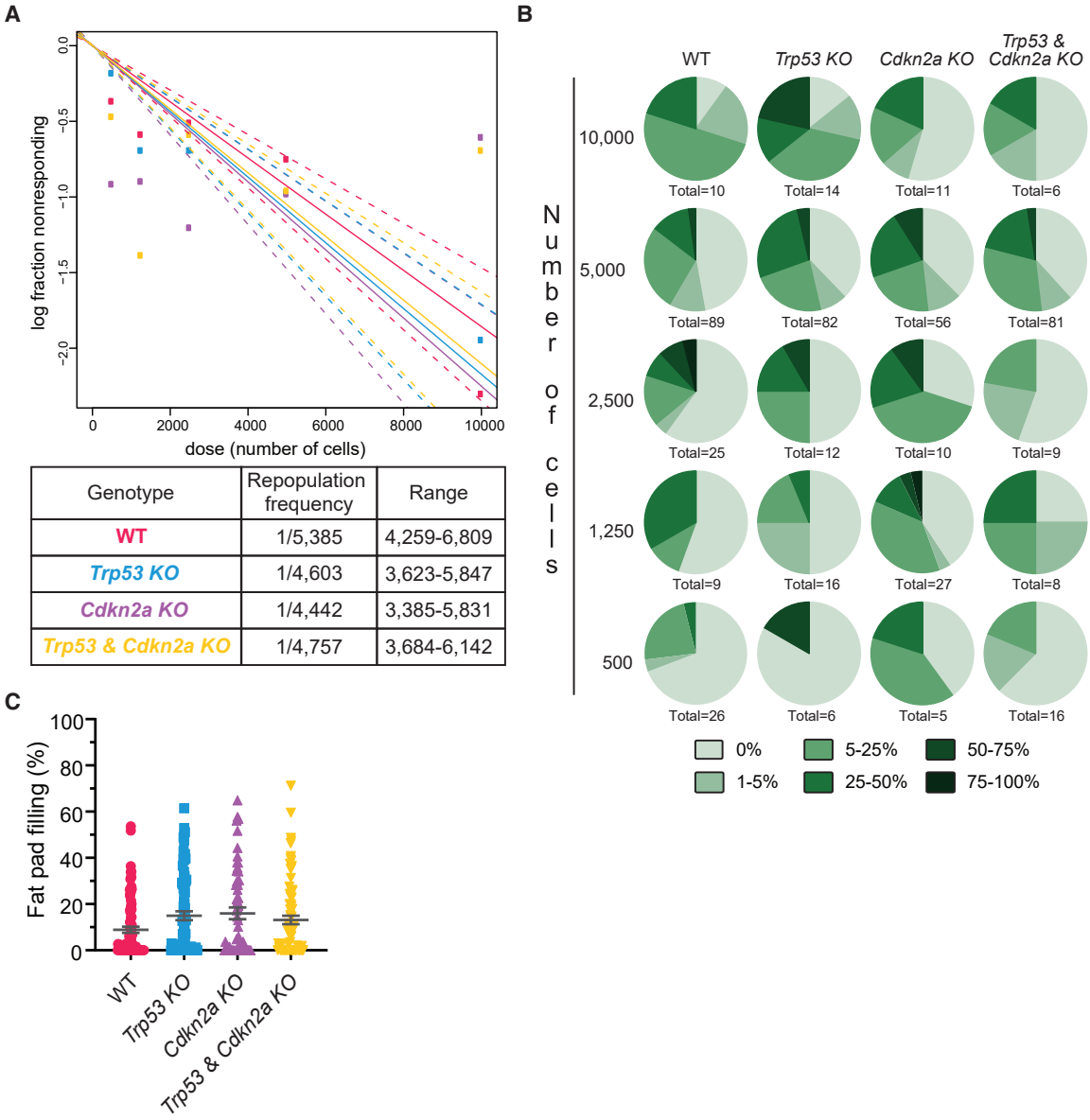

Genotype	Repopulation frequency	Range
WT	1/5,385	4,259-6,809
Trp53 KO	1/4,603	3,623-5,847
Cdkn2a KO	1/4,442	3,385-5,831
Trp53 & Cdkn2a KO	1/4,757	3,684-6,142

Figure 2. WT, *Trp53 KO*, *Cdkn2a KO*, and *Trp53 & Cdkn2a KO* MECs Display Equal Short-Term Repopulation Potential

An overview of this experiment is shown in Figure S2.

(A) Extreme limiting dilution analysis results of the limiting dilution transplantation assay. A minimum of 11 donor mice were used for each genotype and data derive from a minimum of four separate experiments for each genotype ($p > 0.05$ for all comparisons).

(B and C) Overview of the data displayed in (A). The number of cells injected, the total number of transplantations performed, and the percentage donor outgrowths occupied in recipient fat pads are shown. In (B) the data are grouped in pie charts. In (C) the size of the individual outgrowths after 5,000 cells were injected is shown. Data are presented as mean ± SEM; each symbol represents one transplant ($p > 0.05$ for all comparisons; one-way ANOVA). Plots similar to those displayed in (C) for other injected cell numbers are shown in Figure S3.

derived from WT (1/5,385), *Trp53 KO* (1/4,603), *Cdkn2a KO* (1/4,442), and *Trp53 & Cdkn2a KO* (1/4,757) glands (Figures 2A and 2B). Moreover, analysis of the size of the regenerated donor glands also showed no differences between the different mouse models (Figures 2C and S3A–S3D). This demonstrates that p53, $p16^{INK4a}$, and $p19^{ARF}$ do not affect the ability of MECs to regenerate or proliferate in a primary transplantation assay.

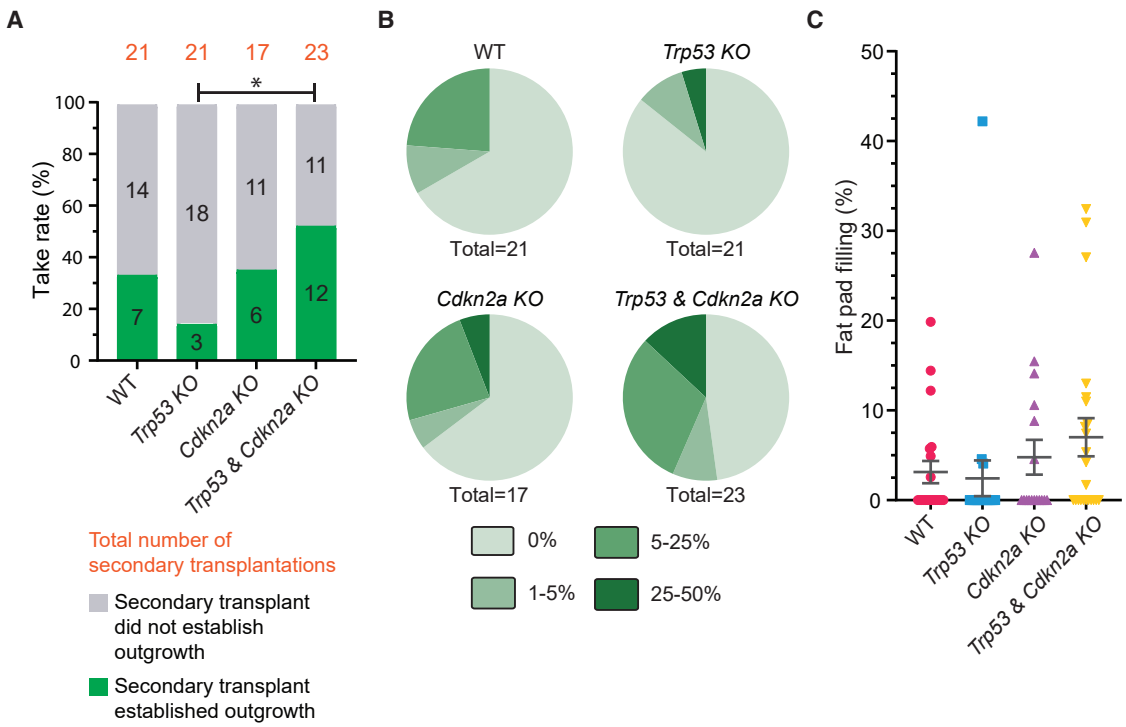

Figure 3. Long-Term Renewal Is Reduced in the Absence of *Trp53* and Rescued by the Depletion of *Cdkn2a*

An overview of this experiment is shown in Figure S2.

(A) The take rate of the secondary transplantation assay. Total number of secondary transplants is shown in orange, positive outgrowths are shown in green, no outgrowths are shown in gray (*$p < 0.05$; Fisher's exact test).

(B and C) Overview of the data displayed in (A). The total number of transplantations and the percentage donor outgrowths occupied in recipient fat pads are shown. In (B) the data are grouped in pie charts. In (C) the size of individual outgrowths is shown. Data are presented as mean ± SEM; each symbol represents one transplant ($p > 0.05$ for all comparisons; one-way ANOVA).

The Absence of *Trp53* Reduces Secondary Transplant Repopulation Frequency Compared with *Trp53 & Cdkn2a KO* MECs

To investigate if the deletion of *Trp53* and/or *Cdkn2a* leads to changes in the ability to self-renew and/or proliferate long term, secondary transplantations were performed (Figure S2). WT, *Cdkn2a KO*, and *Trp53 & Cdkn2a KO* MECs showed similar frequencies of long-term self-renewing cells, as did WT, *Trp53 KO*, and *Cdkn2a KO* MECs. Meanwhile, *Trp53 & Cdkn2a KO* MECs showed a significantly higher regeneration frequency compared with *Trp53 KO* MECs (Figure 3A); therefore, the ablation of *Cdkn2a* appears to rescue long-term self-renewal capacity in the *Trp53 & Cdkn2a KO* MECs. The deletion of any of the tumor suppressor genes did not affect the rate of proliferation (Figures 3B and 3C).

Trp53 & Cdkn2a KO Luminal Progenitor MECs Do Not Regenerate when Transplanted

In the hematopoietic system, *Trp53 & Cdkn2a KO* multipotent progenitors acquire the capacity to self-renew and regenerate the blood system in transplantation experiments (Akala et al., 2008). To investigate if in the mammary gland *Trp53 & Cdkn2a KO* progenitors also possess such capabilities, we used fluorescence-activated cell sorting (FACS) to select for progenitors and transplant them in syngeneic mice. Prior to this experiment, we corroborated published data showing that the luminal cells encompass a progenitor cell population that expresses the cell surface marker CD14 (Asselin-Labat et al., 2011). *In vitro*, luminal $CD14^+$ cells form more organoids than $CD14^-$ luminal cells, confirming that CD14 enriches strongly for luminal progenitors (Figure S4A). Subsequently, we performed a limiting dilution assay with WT and *Trp53 & Cdkn2a KO* luminal $CD14^+$ progenitors; none of these transplantations resulted in the regeneration of the mammary epithelium (Figure S4B). Thus, p53, $p16^{INK4a}$, and $p19^{ARF}$ do not or are not sufficient to inhibit luminal $CD14^+$ progenitors from self-renewing in transplantation assays.

Trp53 & Cdkn2a KO Basal MECs Are Sensitized to TNF-α-Induced Proliferation

Last, we compared gene expression between WT and *Trp53 & Cdkn2a KO* mice. Considering that luminal progenitors

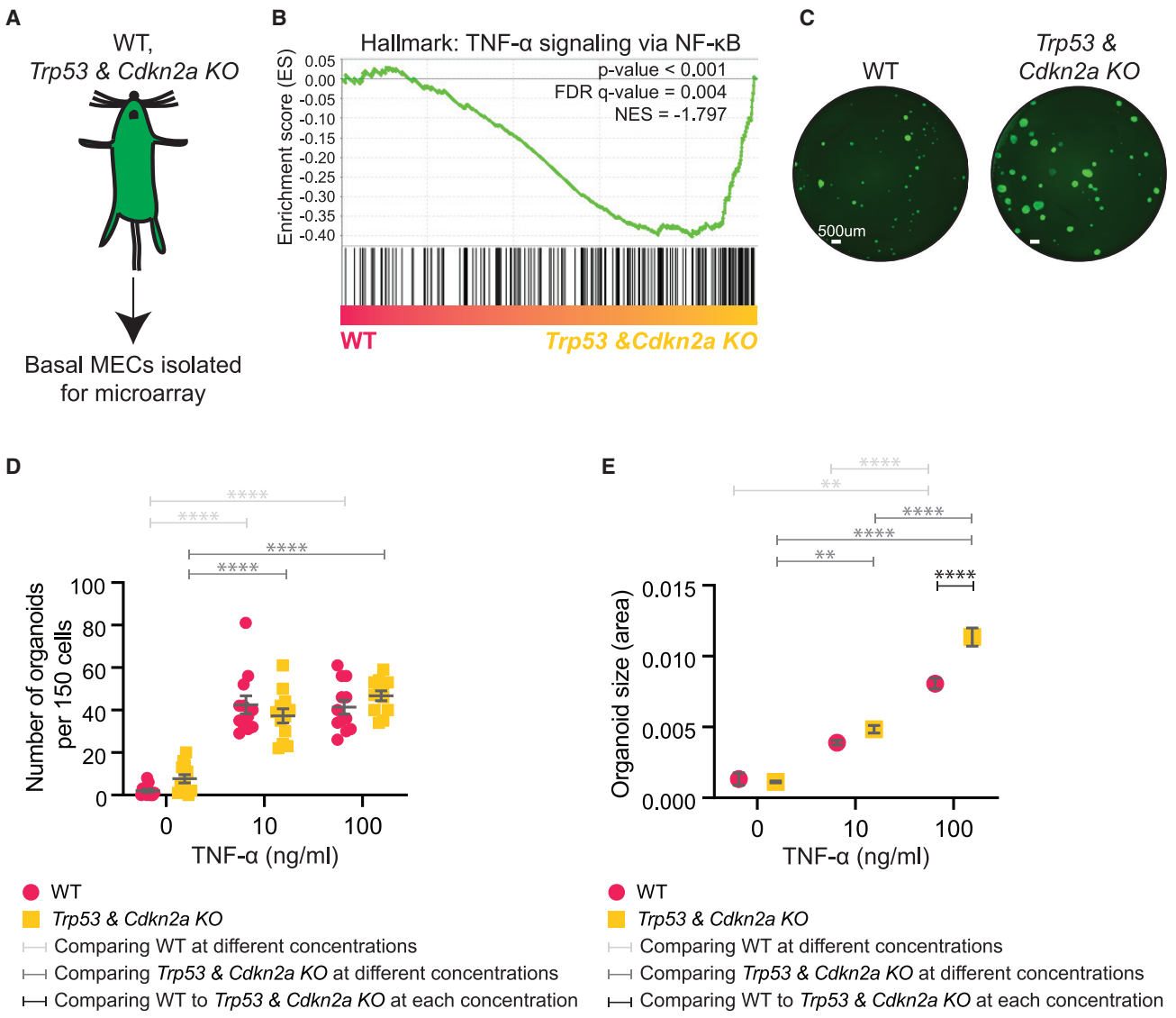

Figure 4. *Trp53 & Cdkn2a KO* Basal MECs Are Sensitized to TNF-α-Induced Proliferation

(A) An overview of WT and *Trp53 & Cdkn2a KO* basal MECs that were sorted using FACS to isolate RNA for RNA microarray expression analysis.

(B) GSEA results of the hallmark gene set TNF-α via NF-κB of WT and *Trp53 & Cdkn2a KO* basal MECs. Three biological replicates of each genotype were analyzed. All significant GSEA results are shown in Table S1.

(C) Fluorescence image of an *in vitro* organoid formation assay showing 150 WT or *Trp53 & Cdkn2a KO* basal cells treated with TNF-α. Photos shown are examples of wells treated with 100 ng/mL TNF-α for 2 weeks.

(D and E) Plots show the number (D) and size (E) of organoids that had formed after 150 WT and *Trp53 & Cdkn2a KO* basal MECs were cultured for 2 weeks in the presence of 0, 10, or 100 ng/mL TNF-α. Data from four biological replicates and three technical replicates are displayed. In (D), the number of organoids counted in each well is displayed (n = 12 wells). In (E), the symbol shows the mean organoid size. Data are presented as mean ± SEM. Two-way ANOVA compares WT basal MECs in the presence of different concentrations of TNF-α in light gray, *Trp53 & Cdkn2a KO* basal MECs at different concentrations of TNF-α in dark gray, and WT to *Trp53 & Cdkn2a KO* basal MECs at each concentration of TNF-α in black (**p < 0.01; ****p < 0.0001; two-way ANOVA).

do not regenerate *in vitro* (Figure S4B), we focused on basal MECs. WT and *Trp53 & Cdkn2a KO* basal MECs were sorted using FACS, and their respective RNAs were extracted and submitted for RNA microarray analysis (Figure 4A). Gene set enrichment analysis (GSEA) revealed that TNF-α signaling via NF-κB was enhanced in *Trp53 & Cdkn2a KO* basal MECs (Figure 4B and Table S1). TNF-α is a cytokine released by immune cells, predominantly by macrophages. Upon binding to a receiving cell, it can stimulate cell survival or cell death depending on other actors in the cell.

When the TNF-α signaling cascade activates the transcription factor complex NF-κB, NF-κB stimulates cellular survival by increasing proliferation and inflammation (Ting and Bertrand, 2016). To investigate if TNF-α affects the growth of basal MECs, we exposed WT and *Trp53 & Cdkn2a KO* basal MECs to different concentrations of TNF-α in an organoid formation assay. Exposure to TNF-α led to an increase in organoid number and size, regardless of genotype (Figures 4C–4E). The number of organoids formed upon TNF-α exposure was similar between WT and *Trp53 & Cdkn2a KO* basal MECs and did not change as the concentration of TNF-α increased (Figure 4D). Notably, *Trp53 & Cdkn2a KO* basal MEC organoids grew significantly larger than their WT counterpart when exposed to 100 ng/mL TNF-α (Figure 4E). Thus, while TNF-α stimulates the formation and proliferation of both WT and *Trp53 & Cdkn2a KO* basal MEC organoids equally, organoids derived from *Trp53 & Cdkn2a KO* basal MECs were larger in size.

DISCUSSION

In this report, we set out to understand the molecular mechanisms that regulate self-renewal and proliferation in the epithelium of the mammary gland. We focused on the roles of p53, $p16^{INK4a}$, and $p19^{ARF}$, as they have been reported to play an important role in the suppression of hematopoietic self-renewal and proliferation (Akala et al., 2008). Unlike the hematopoietic system, we find that p53, $p16^{INK4a}$, and $p19^{ARF}$ do not regulate short-term self-renewal or proliferation in C57BL/6J mice. Interestingly, we found that *Trp53 KO* MECs in these mice show a lower long-term regeneration ability than *Trp53 & Cdkn2a KO* MECs. This is in line with the report that loss of $p16^{INK4a}$, rather than *Trp53*, contributes to the self-renewal of quiescent mammary stem cells (Cai et al., 2017). On the other hand, long-term self-renewal is similar between *Trp53 KO*, WT, and *Cdkn2a KO* MECs. Furthermore, ablation of any of these tumor-suppressor genes does not affect proliferation in secondary transplantations. Therefore, we conclude that overall, p53, $p16^{INK4a}$, and $p19^{ARF}$ do not play a significant role in mammary gland self-renewal or are not sufficient to regulate mammary gland self-renewal.

Previously, other groups have examined the effects of these three tumor suppressors on mammary epithelium self-renewal using transplantation assays. In accordance with what we report, Pietersen et al. found that WT and $Cdkn2a^{-/-}$ MECs have the same number of self-renewing cells (Pietersen et al., 2008). The three groups that studied p53 and mammary gland self-renewal found an increase in self-renewing cells in the absence of *Trp53*. Two groups used different mouse strains in their studies (Chiche et al., 2013; Tao et al., 2011). It has been widely reported that the use of different mouse strains can affect results (Rivera and Tessarollo, 2008). A third group also reported on the increase in self-renewal in $Trp53^{-/-}$ MECs, using a C57BL/6J *Trp53* null mouse (Cicalese et al., 2009), in contrast to our conditional C57BL/6J *Trp53 KO* model, where *Trp53* is absent in only a subset of cells. Moreover, after digestion, Cicalese et al. transplanted all remaining cells of the mammary fat pad, including $Trp53^{-/-}$ stromal cells, whereas we used FACS to select for MECs. In the case of cancer, stromal cells can stimulate tumor growth by silencing p53 (Bar et al., 2010). This raises the possibility that the loss of p53 in stromal cells influences mammary stem cell frequency. It would be interesting to investigate the repopulation frequency of *Trp53* null and conditional *Trp53 KO* glands in a WT and *Trp53* null environment to answer this question. To corroborate the reliability of our data, we used FACS to select for GFP^+ MECs, whereby once transplanted, the color marker facilitated the identification of transplanted donor cells among the colorless cells in recipient mice.

In our mouse model we make use of the *Krt14-Cre* transgenic mouse. It is important to note that normal mammary development has been reported in this transgenic strain (Mitchell and Serra, 2014). However, *Cre* expression can result in unintentional effects. For example, in a different *Krt14-Cre* inducible mouse, tetraploid keratinocytes form in the skin (Janbandhu et al., 2014). To limit potential misinterpretation of our data, all four mouse models in this study expressed *Krt14-Cre* and at least one target *loxP* site. Moreover, our WT (1/5,385) limiting dilution data show a frequency similar to that of C57BL/6J WT cells (1/9,045) (Scheeren et al., 2014), noting that due to the absence of a mammary epithelial marker, Scheeren et al. included stromal cells, resulting in a decreased frequency compared with our WT mice.

Unlike the hematopoietic multipotent progenitor, we find that mammary luminal progenitors do not acquire the ability to self-renew. It remains possible that we did not transplant enough cells to find a regenerating *Trp53 & Cdkn2a KO* $CD14^+$ luminal progenitor, but if one does arise in the mutant progenitor it is very rare. Another possibility is the existence of a different mammary progenitor cell type, not marked by luminal $CD14^+$, which is sensitive to the ablation of *Trp53*, $p16^{INK4a}$, and $p19^{ARF}$. If this is true, unlike in the hematopoietic system, such a mutated cell does not affect self-renewal significantly, since the repopulation frequency is not affected in primary transplants.

Comparing WT and *Trp53 & Cdkn2a KO* basal MEC transcriptional data, we found an enhancement of TNF-α signaling via the NF-κB pathway in the *Trp53 & Cdkn2a KO* basal MECs. We validated these results by exposing WT and *Trp53 & Cdkn2a KO* basal MECs to TNF-α *in vitro*. TNF-α exposure strongly increased the number of basal

MECs growing out into organoids and their ability to proliferate. While TNF-α equally affected organoid number, it resulted in enhanced proliferation in *Trp53 & Cdkn2a KO* basal MECs. In the rat mammary gland, TNF-α induces cellular proliferation as well (Ip et al., 1992). In mice, TNF-α exposure activates NF-κB, enabling the epithelial cells of the liver, the hepatocytes, to be extensively passaged *in vitro* and even subsequently engrafted *in vivo* (Peng et al., 2018). Molecularly, $p16^{INK4a}$, $p19^{ARF}$, and p53 can interact with NF-κB. $p16^{INK4a}$ and $p19^{ARF}$ can suppress the transcriptional activity of the NF-κB complex (Rocha et al., 2003). The literature on p53 and NF-κB is more extensive, describing how p53 can modulate NF-κB (Perkins, 2012). In contrast, mutant p53 can disrupt modulation, increasing and strengthening NF-κB activity to promote proliferation and tumorigenesis (Weisz et al., 2007). NF-κB activation is involved with various cancer hallmarks, but most notably with inflammation, often induced by TNF-α (Taniguchi and Karin, 2018). TNF-α is highly expressed in macrophages, and macrophages are part of the stromal niche of the mammary gland. Eliminating macrophages impairs mammary gland development and mammary stem cell self-renewal (Chakrabarti et al., 2018). Our data indicate that losing tumor suppressors p53, $p16^{INK4a}$, and $p19^{ARF}$ makes mammary cells more prone to excessive proliferation in the presence of inflammation. Therefore, our data highlight the importance of controlling inflammation to slow down the mutation-prone overproliferation and the subsequent oncogenic transformation when mammary stem cells lose their genome guard p53 and senescence triggers $p16^{INK4a}$ and $p19^{ARF}$.

EXPERIMENTAL PROCEDURES

Animal Care and Use

Mice were purchased from The Jackson Laboratory: *Trp53*$^{f/f}$ (Stock 008462), *Krt-14-Cre* (Stock 004782), *mT/mG* (Stock 007676), and weaning-aged transplantation recipients C57BL/6J (Stock 000664). From the NCI Mouse Repository we purchased *Cdkn2a* null (Stock 01XB1) mice. All mice were females and backcrossed into the C57BL/6J background for at least six generations. All mice used for this study were maintained at the Stanford Veterinary Service Center in accordance with the guidelines of the Administrative Panel on Laboratory Animal Care (APLAC 10868).

Tissue Processing and FACS

Mammary fat pads from adult virgin mice were surgically resected, digested, and filtered to obtain a single-cell suspension. In between digestion steps and prior to FACS, cells were kept in HBSS (catalog No. 21022CV, Corning) + 2% FBS (catalog No. FB-01, Omega Scientific) + PSA (catalog No. 15240112, Gibco). Cells were stained with fluorophore-attached antibody and DAPI for FACS.

Transplantations

Cells, counted with a hemocytometer, in HBSS + 2% FBS + PSA were mixed with 50% Matrigel (catalog No. 356234, Corning) were injected at 10 μl into a cleared fat pad of a weaning-age mouse, as previously described (Cai et al., 2017). Secondary transplants were performed as shown in Figure S2. After at least 7 weeks, transplants were dissected and photographed using a fluorescence microscope.

Mammary Organoid Growth Assay

Cells were plated in a 96-well plate on growth-factor-reduced Matrigel (catalog No. 354230, Corning) in culture medium, which is described in the Supplemental Experimental Procedures.

RNA Extraction

Using FACS, cells were directly sorted into RNAprotect (catalog No. 76526, Qiagen). RNA was extracted using the RNeasy micro kit (catalog No. 74004, Qiagen), according to the manufacturer's instructions.

RNA Microarray and RNA Microarray Data Analysis

Library preparation, hybridization, and scanning were all performed by the Stanford protein and nucleic acid facility (PAN facility) using the Mouse Gene 2.0 ST Array (catalog No. 902118, Affymetrix). Data were analyzed using Transcriptome Analysis Console Software (Thermo Fisher Scientific). Patterns in gene expression were analyzed using GSEA v.4.0.1 (Mootha et al., 2003; Subramanian et al., 2005) and the hallmark gene sets (Liberzon et al., 2015).

Quantification and Statistical Analysis

Statistical tests used are indicated in the figure legends; data are presented as the mean ± SEM. Determination of transplant size is explained in Figure S2. The frequency of repopulating cells in the primary transplantation assay was calculated using ELDA (Hu and Smyth, 2009). To count organoid number and size, images taken from each experiment were processed simultaneously. Photoshop CS6's threshold function removed background noise to show only organoids; this allowed for automated counting and size analysis. Subsequently, using ImageJ v.1.51, we used Analyze Particles to count and measure the size of the organoids. All graphs were made in Prism 8. FACS data were analyzed in FlowJo v.10.

Data and Code Availability

Microarray expression data (GEO: GSE137573) are available in the Gene Expression Omnibus.

SUPPLEMENTAL INFORMATION

Supplemental Information can be found online at https://doi.org/10.1016/j.stemcr.2020.12.012.

AUTHOR CONTRIBUTIONS

Conceptualization, L.J.v.W., F.A.S., and M.F.C.; Methodology, L.J.v.W., F.A.S., S.C., and M.F.C.; Investigation, L.J.v.W., D.Q., and W.H.D.H.; Formal Analysis, L.J.v.W.; Writing – Original Draft,

L.J.v.W.; Writing – Review & Editing, all authors; Funding Acquisition, M.F.C.

ACKNOWLEDGMENTS

This work was supported by Breast Cancer Research Foundation grant (BCRF-18-027), the Ludwig Cancer Research Foundation, and a CIRM Bridges award (to W.H.D.H.). Some research was performed on a FACSAriaII that was purchased using an NIH S10 shared instrumentation grant (1S10RR02933801). We thank Amy Doan for help with mouse maintenance and the Stanford Veterinary Service Center for providing mouse care; Dr. Lauren E. Grosberg for help with statistical analysis; Dr. Roel Nusse for providing L1-Wnt3a feeder cells; Patty Lovelace, Jennifer Ho, Stephen Weber, Catherine Carswell Crumpton, and Cheng Pan for management of the flow cytometry facility; and Natalia Kosovilka and the Stanford PAN facility for microarray services.

Received: September 25, 2019
Revised: December 18, 2020
Accepted: December 19, 2020
Published: January 21, 2021

REFERENCES

Akala, O.O., Park, I.K., Qian, D., Pihalja, M., Becker, M.W., and Clarke, M.F. (2008). Long-term haematopoietic reconstitution by Trp53-/-p16Ink4a-/-p19Arf-/- multipotent progenitors. Nature *453*, 228–232.

Asselin-Labat, M.L., Sutherland, K.D., Vaillant, F., Gyorki, D.E., Wu, D., Holroyd, S., Breslin, K., Ward, T., Shi, W., Bath, M.L., et al. (2011). Gata-3 negatively regulates the tumor-initiating capacity of mammary luminal progenitor cells and targets the putative tumor suppressor caspase-14. Mol. Cell Biol. *31*, 4609–4622.

Bar, J., Moskovits, N., and Oren, M. (2010). Involvement of stromal p53 in tumor-stroma interactions. Semin. Cell Dev. Biol. *21*, 47–54.

Cai, S., Kalisky, T., Sahoo, D., Dalerba, P., Feng, W., Lin, Y., Qian, D., Kong, A., Yu, J., Wang, F., et al. (2017). A quiescent Bcl11b high stem cell population is required for maintenance of the mammary gland. Cell Stem Cell *20*, 247–260.e5.

Chakrabarti, R., Celià-Terrassa, T., Kumar, S., Hang, X., Wei, Y., Choudhury, A., Hwang, J., Peng, J., Nixon, B., Grady, J.J., et al. (2018). Notch ligand Dll1 mediates cross-talk between mammary stem cells and the macrophageal niche. Science *360*, eaan4153.

Charni, M., Aloni-Grinstein, R., Molchadsky, A., and Rotter, V. (2017). p53 on the crossroad between regeneration and cancer. Cell Death Differ. *24*, 8–14.

Chiche, A., Moumen, M., Petit, V., Jonkers, J., Medina, D., Deugnier, M.A., Faraldo, M.M., and Glukhova, M.A. (2013). Somatic loss of p53 leads to stem/progenitor cell amplification in both mammary epithelial compartments, basal and luminal. Stem Cells *31*, 1857–1867.

Cicalese, A., Bonizzi, G., Pasi, C.E., Faretta, M., Ronzoni, S., Giulini, B., Brisken, C., Minucci, S., Di Fiore, P.P., and Pelicci, P.G. (2009). The tumor suppressor p53 regulates polarity of self-renewing divisions in mammary stem cells. Cell *138*, 1083–1095.

Dassule, H.R., Lewis, P., Bei, M., Maas, R., and McMahon, A.P. (2000). Sonic hedgehog regulates growth and morphogenesis of the tooth. Development *127*, 4775–4785.

Hu, Y., and Smyth, G.K. (2009). ELDA: extreme limiting dilution analysis for comparing depleted and enriched populations in stem cell and other assays. J. Immunol. Methods *347*, 70–78.

Ip, M.M., Shoemaker, S.F., and Darcy, K.M. (1992). Regulation of rat mammary epithelial cell proliferation and differentiation by tumor necrosis factor-alpha. Endocrinology *130*, 2833–2844.

Janbandhu, V.C., Moik, D., and Fässler, R. (2014). Cre recombinase induces DNA damage and tetraploidy in the absence of loxP sites. Cell Cycle *13*, 462–470.

Jonkers, J., Meuwissen, R., van der Gulden, H., Peterse, H., van der Valk, M., and Berns, A. (2001). Synergistic tumor suppressor activity of BRCA2 and p53 in a conditional mouse model for breast cancer. Nat. Genet. *29*, 418–425.

Lessard, J., and Sauvageau, G. (2003). Bmi-1 determines the proliferative capacity of normal and leukaemic stem cells. Nature *423*, 255–260.

Liberzon, A., Birger, C., Thorvaldsdóttir, H., Ghandi, M., Mesirov, J.P., and Tamayo, P. (2015). The Molecular Signatures Database (MSigDB) hallmark gene set collection. Cell Syst. *1*, 417–425.

Lowe, S.W., and Sherr, C.J. (2003). Tumor suppression by Ink4a-Arf: progress and puzzles. Curr. Opin. Genet. Dev. *13*, 77–83.

Mitchell, E.H., and Serra, R. (2014). Normal mammary development and function in mice with Ift88 deleted in MMTV- and K14-Cre expressing cells. Cilia *3*, 4.

Mootha, V.K., Lindgren, C.M., Eriksson, K.F., Subramanian, A., Sihag, S., Lehar, J., Puigserver, P., Carlsson, E., Ridderstråle, M., Laurila, E., et al. (2003). PGC-1alpha-responsive genes involved in oxidative phosphorylation are coordinately downregulated in human diabetes. Nat. Genet. *34*, 267–273.

Muzumdar, M.D., Tasic, B., Miyamichi, K., Li, L., and Luo, L. (2007). A global double-fluorescent Cre reporter mouse. Genesis *45*, 593–605.

Park, I.K., Qian, D., Kiel, M., Becker, M.W., Pihalja, M., Weissman, I.L., Morrison, S.J., and Clarke, M.F. (2003). Bmi-1 is required for maintenance of adult self-renewing haematopoietic stem cells. Nature *423*, 302–305.

Peng, W.C., Logan, C.Y., Fish, M., Anbarchian, T., Aguisanda, F., Álvarez-Varela, A., Wu, P., Jin, Y., Zhu, J., Li, B., et al. (2018). Inflammatory cytokine TNFα promotes the long-term expansion of primary hepatocytes in 3D culture. Cell *175*, 1607–1619.e5.

Perkins, N.D. (2012). The diverse and complex roles of NF-κB subunits in cancer. Nat. Rev. Cancer *12*, 121–132.

Pietersen, A.M., Evers, B., Prasad, A.A., Tanger, E., Cornelissen-Steijger, P., Jonkers, J., and van Lohuizen, M. (2008). Bmi1 regulates stem cells and proliferation and differentiation of committed cells in mammary epithelium. Curr. Biol. *18*, 1094–1099.

Rivera, J., and Tessarollo, L. (2008). Genetic background and the dilemma of translating mouse studies to humans. Immunity *28*, 1–4.

Rizo, A., Olthof, S., Han, L., Vellenga, E., de Haan, G., and Schuringa, J.J. (2009). Repression of BMI1 in normal and leukemic

human CD34(+) cells impairs self-renewal and induces apoptosis. Blood *114*, 1498–1505.

Rocha, S., Campbell, K.J., and Perkins, N.D. (2003). p53- and Mdm2-independent repression of NF-kappa B transactivation by the ARF tumor suppressor. Mol. Cell *12*, 15–25.

Scheeren, F.A., Kuo, A.H., van Weele, L.J., Cai, S., Glykofridis, I., Sikandar, S.S., Zabala, M., Qian, D., Lam, J.S., Johnston, D., et al. (2014). A cell-intrinsic role for TLR2-MYD88 in intestinal and breast epithelia and oncogenesis. Nat. Cell Biol. *16*, 1238–1248.

Serrano, M., Lee, H., Chin, L., Cordon-Cardo, C., Beach, D., and DePinho, R.A. (1996). Role of the INK4a locus in tumor suppression and cell mortality. Cell *85*, 27–37.

Subramanian, A., Tamayo, P., Mootha, V.K., Mukherjee, S., Ebert, B.L., Gillette, M.A., Paulovich, A., Pomeroy, S.L., Golub, T.R., Lander, E.S., et al. (2005). Gene set enrichment analysis: a knowledge-based approach for interpreting genome-wide expression profiles. Proc. Natl. Acad. Sci. U S A *102*, 15545–15550.

Sun, P., Yuan, Y., Li, A., Li, B., and Dai, X. (2010). Cytokeratin expression during mouse embryonic and early postnatal mammary gland development. Histochem. Cell Biol. *133*, 213–221.

Taniguchi, K., and Karin, M. (2018). NF-κB, inflammation, immunity and cancer: coming of age. Nat. Rev. Immunol. *18*, 309–324.

Tao, L., Roberts, A.L., Dunphy, K.A., Bigelow, C., Yan, H., and Jerry, D.J. (2011). Repression of mammary stem/progenitor cells by p53 is mediated by Notch and separable from apoptotic activity. Stem Cells *29*, 119–127.

Ting, A.T., and Bertrand, M.J.M. (2016). More to life than NF-κB in TNFR1 signaling. Trends Immunol. *37*, 535–545.

Van Keymeulen, A., Rocha, A.S., Ousset, M., Beck, B., Bouvencourt, G., Rock, J., Sharma, N., Dekoninck, S., and Blanpain, C. (2011). Distinct stem cells contribute to mammary gland development and maintenance. Nature *479*, 189–193.

Weisz, L., Damalas, A., Liontos, M., Karakaidos, P., Fontemaggi, G., Maor-Aloni, R., Kalis, M., Levrero, M., Strano, S., Gorgoulis, V.G., et al. (2007). Mutant p53 enhances nuclear factor kappaB activation by tumor necrosis factor alpha in cancer cells. Cancer Res. *67*, 2396–2401.